MITSUBISHI ELECTRIC RESEARCH LABORATORIES
http://www.merl.com

Opportunistic Cell Edge Selection in Multi-Cell OFDMA Networks

Chun Kin Au-Yeung, Amine Maaref, Jinyun Zhang

TR2009-092 December 2009

Abstract

We propose an intercell downlink orthogonal frequency division multiple access (OFDMA) scheduling technique in a sectorized cellular network. Adjacent sectors from neighboring cells form a cluster and each OFDMA resource block is allocated to the rate-maximizing sector. Compared to a cellular network that uses conventional fractional frequency reuse (FFR) technique, our proposed system requires only slightly more backhaul traffic while providing an appreciable performance gain. Intercell scheduling, which grants a resource exclusively to the rate-maximizing cell within a cluster is a simple and powerful base station cooperation technique that balances non-cooperation and full cooperation. We find out that a tri-sectored network is particularly well-suited to applying inter-sector scheduling as each cluster is relatively isolated from other clusters. We provide an option to adjust the load on backhaul traffic by adjusting the granularity of the OFDMA resource under contention. We also provide an option to optimally swap resources. Analysis on performance gain for a few configurations are given. Simulations are provided to verify and illustrate the claimed performance gain.

Globecom 2009

Opportunistic Cell Edge Selection in Multi-cell OFDMA Networks

Chun Kin Au-Yeung[†], Amine Maaref[‡] and Jinyun Zhang[‡]
[†]School of Electrical and Computer Engineering, Purdue University
465 Northwestern Ave., West Lafayette, IN 47905
E-mail: cauyeung@purdue.edu
[‡]Mitsubishi Electric Research Laboratories
201 Broadway Cambridge, MA 02139
E-mail: {maaref, jzhang}@merl.com

***Abstract*—We propose an intercell downlink orthogonal frequency division multiple access (OFDMA) scheduling technique in a sectorized cellular network. Adjacent sectors from neighboring cells form a cluster and each OFDMA resource block is allocated to the rate-maximizing sector. Compared to a cellular network that uses conventional fractional frequency reuse (FFR) technique, our proposed system requires only slightly more backhaul traffic while providing an appreciable performance gain. Intercell scheduling, which grants a resource exclusively to the rate-maximizing cell within a cluster, is a simple and powerful base station cooperation technique that balances non-cooperation and full cooperation. We find out that a tri-sectored network is particularly well-suited to applying inter-sector scheduling as each cluster is relatively isolated from other clusters. We provide an option to adjust the load on backhaul traffic by adjusting the granularity of the OFDMA resource under contention. We also provide an option to optimally swap resources. Analysis on performance gain for a few configurations are given. Simulations are provided to verify and illustrate the claimed performance gain.**

***Index Terms*—Inter-sector scheduling, improved FFR, opportunistic OFDMA**

I. Introduction

To meet the ever-increasing transmission rate requirements, base station cooperation is gaining traction as a candidate technology that shows substantial benefit over a non-cooperating cellular network. Many base station cooperation techniques treat the cellular network or the cooperative segment as an augmented multiple antenna system where a group of base stations cooperatively transmit data to a group of selected users in the network [1]–[5]. This level of cooperation results in significant performance gain at the expense of implementation complexity. Since cooperating base stations need to share channel state information (CSI) and data streams, the extra requirement in backhaul traffic is nontrivial. Extra backhaul traffic will likely be supported in future generations of wireless standards but unlikely to be in the recent future.

Cooperating base stations sharing CSI but not data streams is a more likely near-term base station cooperation possibility. This way, each user is served by the same base station as when base stations do not cooperate. Intercell scheduling, proposed in [6], is a technique whereby the entire available spectrum is given to the rate-maximizing base station within a cluster. [6] showed that such a scheme outperforms traditional frequency reuse by an expanded multiuser diversity.

In this paper, we focus our attention in a tri-sectored cellular downlink orthogonal frequency division multiple access (OFDMA) network that uses fractional frequency reuse (FFR). Multicell OFDMA resource allocation attracts a body of literature (e.g. [7]) using various assumptions. In an FFR system, mobile user equipment (UE) is categorized as either a cell-center UE or a cell-edge UE. The available spectrum is divided into two non-overlapping segments, one for serving cell-center UEs and the other for cell-edge UEs. We then apply inter-sector scheduling in the spirit of [6] where each OFDMA resource block (RB) in the cell-edge segment is given to the rate-maximizing sector without restricting, though it is an option, to give the winning sector exclusive access to the entire spectrum. Every sector serves its cell-center users using cell-center RBs. We find that a tri-sectored OFDMA network is particularly suited to apply our proposed scheme since interference from neighboring clusters is substantially mitigated by the sectorized architecture and the resource allocation granularity that OFDMA provides. Moreover, only the highest achievable data rates need to be shared for each competing sector, which is normally available in schemes without base station cooperation. No extra CSI feedback is required from the mobile terminals beyond what is needed in a non-cooperating system. These two properties make inter-sector scheduling an attractive solution to improving any sectorized FFR based network with minimal change. Comparing with [7] where every UE's achievable rate on each RB is made available to the scheduler, our proposed scheme trades off a little performance for a significant reduction in backhaul signaling. We further provide two variations to our scheme. The first groups cell-edge RBs in a batch and the latter is allocated to the rate-maximizing sector. This variation trades off performance for even lower backhaul traffic. In the second variation, three RB batches are assigned at a time, where each sector is assigned exactly one RB batch. This ensures a level of fairness at the sector scheduling level.

The rest of this paper is organized as follows. Section II details our system layout and basic assumptions. Section

This work was done while Chun Kin Au-Yeung was a graduate intern at Mitsubishi Electric Research Laboratories (MERL).

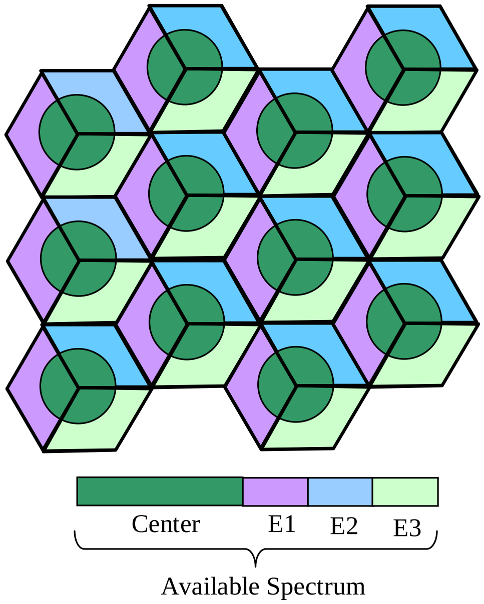

Fig. 1. Fractional frequency reuse layout for 3-sector cellular network.

III describes our opportunistic cell edge selection scheme. Section IV provides some analytical insights into our proposed scheme. Finally, section V validates our results with simulations while section VI provides concluding remarks and future directions.

II. System Setup

We consider a tri-sectored hexagonal cellular downlink network where each sector is served by a base station with three collocated directional antennas, each serving its respective sector. Each sector is further partitioned into a sector center region, which is geographically closer to the base station, and a sector edge region, which is geographically further away from the serving base station. An example architecture with this set of assumptions is the FFR system. A sample spectrum planning for a tri-sectored FFR system is shown in Fig. 1. In a typical sectorized FFR setup, the available frequency spectrum is divided into four non-overlapping bands: one band for serving sector center UEs (center band) and three bands for serving sector edge UEs (edge band). As inter-sector (same cell and out of cell) interference for center region UEs is relatively small, center band is reused in every sector. Edge UEs experience more interference and thus edge bands are mapped similar to a traditional frequency reuse system with a reuse factor of three. As shown in Fig. 1, every cell uses the entire spectrum either to serve its center UEs or to serve its edge UEs in one of its three sectors. In an orthogonal frequency division multiple access (OFDMA) system, the available spectrum is divided into multiple mutually orthogonal groups of subcarriers, often referred to as resource blocks (RB). RBs are assigned to UEs in each cell in a way that no intracell interference occurs. Typically neighboring sectors do not use the same edge bands to reduce cell edge interference.

Let there be K UEs per sector and B base stations in the entire network. There are $3B$ sectors in a tri-sectored network and we number the sectors from 1 to $3B$ such that sectors $3\beta-2, 3\beta-1, 3\beta$ belong to cell β. We denote the sector that UE k resides in as sector $b(k)$. Let there be C OFDMA RBs in total. Let C_c denote the number of cell center RBs per sector, then there are $C_e = (C - C_c)/3$ average number of edge RBs per sector.

On RB $c, c = 1, \ldots, C$, the input-output relationship for UE $k, k = 1, \ldots, K$, has a baseband representation of

$$y_k^c = H_{b(k)k}^c x_{b(k)}^c + \sum_{b=1, b \neq b(k)}^{3B} H_{bk}^c I(b(k), c) x_b^c + n_k^c \ , \quad (1)$$

where y_k^c is mobile k's complex received symbol on RB c, H_{bk}^c is the equivalent complex channel coefficient from sector b to UE k on RB c, $I(b, c)$ is an indicator function that maps to one when sector b is scheduled to use RB c and zero otherwise, x_b^c is the complex transmitted symbol from sector b's transmitter on RB c, and finally n_k is the additive white Gaussian noise (AWGN) experienced at mobile k. For each sector, we impose the average power constraint of $E(|x_b^c|^2) \leq P$. Additive noise is modeled as a complex circularly symmetric Gaussian random variable, i.e. $n_k^c \sim \mathcal{CN}(0, 1)$. We assume that the channel coefficients H_{bk}^c are independent and identically distributed (i.i.d.) for $b = 1, \ldots, 3B$ and for $k = 1, \ldots, K$.

We further assume that each UE estimates the channel coefficients H_{bk}^c for $b = 1, \ldots, 3B$ and $c = 1, \ldots, C$ perfectly. A block fading channel model is adopted whereby the channel remains constant for a transmission period and then independently changes to another value in the next transmission period. The existence of an errorless and zero-delay feedback channel from each UE to its serving base station to feedback CSI information is also assumed. CSI represents the channel quality indicator (CQI), which consists of the SINR values for each RB. Similar to current wireless cellular standards, e.g. 3GPP Long-Term Evolution (LTE), a backhaul high-rate wireline channel, referred to as X_2 interface in 3GPP LTE terminology, connects neighboring base stations. It is implicitly assumed that such a backhaul traffic is errorfree, and induces negligible delay.

Our goal is to design a communication scheme where the backhaul allows each base station in a cluster to share only one value for each edge RB, and allocate each edge RB to only one base station in the cluster, similar to the conventional FFR scheme. Opportunistic cell edge selection, as we discuss in the next section, is the basis of our proposed scheme.

III. Opportunistic Cell Edge Selection

A. Background

Intercell scheduling is a simple and versatile form of base station cooperation [6]. Instead of pre-assigning each cell with a fixed fraction of the available spectrum, intercell scheduling dynamically allocates the *entire* spectrum to the rate maximizing UE within a cluster. As [6] shows, the expanded user diversity, resulting from an expanded user selection pool, yields a sum rate growth of $\sqrt{\log(K)}$. This significant gain is a result of the larger channel variation due to shadowing effects, compared to the well known growth rate $\log\log(K)$ on a Rayleigh channel [8].

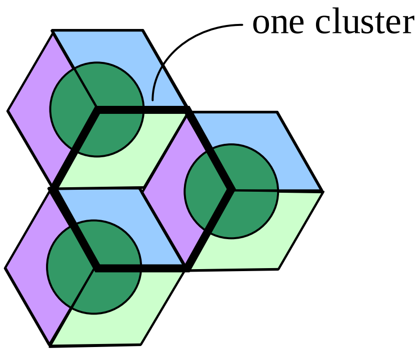

Fig. 2. Cluster in a sectorized cellular layout.

A disadvantage of the scheme in [6] is the possibility that neighboring clusters simultaneously schedule adjacent cells to transmit, thereby effectively reducing the reuse distance compared to the FFR scheme. Fortunately, this disadvantage is substantially mitigated in a sectorized OFDMA cellular network, as interference is largely localized to originate from neighboring sectors of different cells and OFDMA provides finer resource allocation granularity.

B. Opportunistic Cell Edge Selection Algorithm

We define a cluster as three neighboring sectors from three neighboring cells, as shown in Fig. 2. Note that, similar to every cell, every cluster uses all of the available frequency bands. Since UE k has perfect knowledge of $H^c_{b(k)k}$ and $\sum_{b=1,b\neq b(k)}^{3B} |H^c_{bk}|^2$ for $c = 1, \ldots, C$, it calculates the SINR for each RB c by

$$\mathrm{SINR}^c_k = \frac{|H^c_{b(k)k}|^2}{\frac{1}{P} + \sum_{b=1,b\neq b(k)}^{3B} |H^c_{bk}|^2}. \tag{2}$$

For center band RB c and for center UE k, (2) gives the actual operational SINR since every sector reuses RB c. From here on, we focus on edge RB c. In our proposed selection scheme, (2) underestimates the actual SINR when the system is in operation since two-thirds of the sectors will not be transmitting using RB c in operation. Without a priori knowledge of which sectors will be chosen to transmit on RB c, mobile k must estimate this interference. Note that any interference estimate that is a monotonically increasing function of $\sum_{b=1,b\neq b(k)}^{3B} |H^c_{bk}|^2$ will result in the same sector selection outcome (which we will detail shortly) and thus will not affect the performance.

Define $K(b) \triangleq \{k | b(k) = b\}$ to be the UE set that sector b serves, and $C(b) \triangleq \{\text{Sector } b' : b' \text{ in the same cluster as } b\}$ as the group of sectors belonging to the same cluster as b. Sector b determines the UE with the highest reported SINR on RB c and the SINR value by

$$k_c(b) \triangleq \operatorname*{argmax}_{k\in K(b)} \mathrm{SINR}^c_k \tag{3}$$

$$\mathrm{SINR}_c(b) \triangleq \max_{k\in K(b)} \mathrm{SINR}^c_k, \tag{4}$$

for $c = 1, \ldots, 3C_e$. The $3C_e$ SINR values for each sector b are shared with other sectors in $C(b)$. This information sharing can be achieved by either having every sector submitting its SINRs to a central cluster scheduler over the X_2 interface or by having the mobile terminals directly send their SINRs to the other two sectors over the air interface.[1] These two approaches will result in the same scheduler outcome. Knowing the SINRs of the three sectors in the cluster for each edge RB, the scheduler allocates each RB to the rate-maximizing sector; i.e., for cluster $C(b)$, edge RB c is assigned to sector $\operatorname*{argmax}_{b'\in C(b)} \mathrm{SINR}_c(b')$. The other two sectors in $C(b)$ will not use edge RB c. Fig. 3 shows an example of the cellular scheduling layout on a particular edge RB. As shown in the figure, it is possible that neighboring sectors of the same cell simultaneously schedule to use the same RB. This is analogous to the scheduling problem in [6]. Fortunately, due to the directional antenna orientation in a sectorized network, interference is somewhat localized to a cluster.

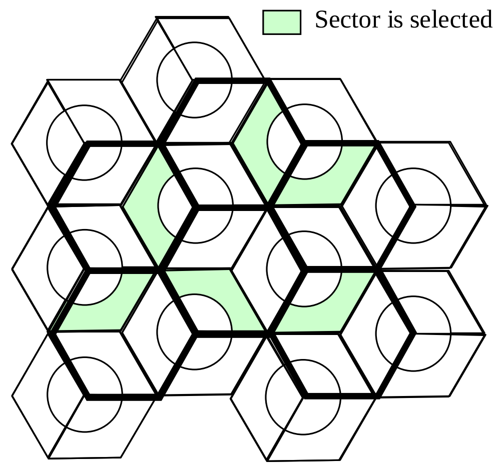

Fig. 3. Sample cellular scheduling layout on an edge RB.

C. Resource Contention Granularity

To some cellular networks, sharing C_e SINR values can put too much strain on the backhaul. Our scheme can address this by grouping multiple RBs in a batch and only share the sum-achievable-rate for the batch. The entire batch of RBs is scheduled to the winning sector. Let there be n_{RB} edge RBs in a RB batch, $1 \leq n_{RB} \leq C_e$. It is possible to have $C_e < n_{RB} \leq 3C_e$, but the performance of such a scheme can be inferior to FFR as it is more restrictive than an FFR scheme. The special case of $n_{RB} = 3C_e$ corresponds to the case where only one sector in a cluster monopolizes all the cell-edge resources of that cluster. Then the additional backhaul strain over the conventional FFR system is $3C_e/n_{RB}$ SINR values per cluster when a central scheduler is used, and $6C_e/n_{RB}$ SINR values per cluster when each sector broadcasts its SINR values to the other two sectors.

D. Fairness

Any scheduling scheme that selects the rate-maximizing UE requires extra mechanisms to prevent resource starvation

[1] Note that both approaches are plausible from a standardization point of view and have their pros and cons.

to the weaker UEs. In this paper, we define RB_{max} as the maximum number of RBs to assign to any given UE in a single scheduling period. As we assume a homogenous UE distribution, this mechanism is suitable for ensuring long term fairness.

As we restrict our attention to schemes where base stations can only share one value per edge RB batch, the independence between each edge RB batch no longer holds for finite RB_{max} and the rate-maximizing allocation scheme is not known. For simplicity, we use a greedy procedure and explain it assuming $n_{RB} = 1$. Sector b shares $\max_{c=1,\ldots,3C_e} \text{SINR}_c(b)$ with other sectors in $C(b)$ and the sector with the largest reported SINR receives the RB allocation. Note that the three sectors may report three SINR values for three different RBs. Only the winning RB is allocated. Each sector then finds the rate-maximizing RB from the remaining RBs, and the process continues until all RBs are allocated, or if all UEs receive $\text{RB}_{\max}$ RBs.

E. RB Rotation

In this variation, three batches of RBs are assigned at a time. The rate-maximizing allocation where each sector gets exactly n_{RB} RBs is chosen. In this way, fairness is built-in and every sector will get exactly C_e edge RBs for each scheduling period. Note that the backhaul requirement of RB rotation is identical to the scheme where each edge RB is assigned to the rate-maximizing sector.

When $n_{RB} = C_e$, the scheduler finds the rate-maximizing band rotation. Note that since sectors have already adhered to the RB_{max} constraint when reporting SINRs to the central scheduler, the scheduling outcome will automatically satisfy the RB_{max} constraint.

IV. Performance Analysis

For mathematical tractability, we only consider $\text{RB}_{\max} = \infty$ in the analysis, i.e., there is no constraint on the number of RBs that can be assigned to a particular UE. For $a > 0$, define the cumulative distribution function (CDF)

$$F_{\text{OCES}}(a) \triangleq P(\text{SINR}_{\text{OCES}} \leq a)$$

and

$$F_{\text{FFR}}(a) \triangleq P(\text{SINR}_{\text{FFR}} \leq a),$$

where $\text{SINR}_{\text{OCES}}$ and SINR_{FFR} are the SINR values on a given edge RB using the proposed opportunistic cell edge selection scheme and FFR, respectively. As interference is largely localized within clusters due to sectorization and assuming a balanced traffic among cells and sectors, it intuitively follows that the distributions of the FFR scheme and the proposed opportunistic scheme can be approximated through the relationship

$$F_{\text{OCES}}(a) \approx F_{\text{FFR}}(a)^3. \tag{5}$$

Note that (5) holds even for $n_{RB} > 1$.

Next we study the RB rotation policy. The exact analysis is quite cumbersome, so we provide the analysis for a greedy-based suboptimal simplification. Again, we assumme $n_{RB} = 1$ for the purpose of this analysis, the extenstion to larger RB batch sizes being trivial. Each scheduler has available nine reported SINR values which consist of reports on each of the three RBs from each of the three sectors in the cluster. The scheduler ranks them in a decreasing order $\text{SINR}^{(1)} \geq \ldots \geq \text{SINR}^{(9)}$ (For simplicity, we define $\text{SINR}^{(0)} = \infty$ and $\text{SINR}^{(10)} = 0$). Table I(a) shows one such ranking of the nine SINR values, where the entries are the rankings. For simplicity, we assume these nine SINR values to be independently and identically generated. Note that for a given sector, the SINRs for different RBs may exhibit strong correlation due to frequency selectivity. In the first step, sector 2 has the highest SINR ranking on RB 3 and is scheduled as shown in Table I(b). Among the unassigned RBs and UEs, sector 1 has the highest SINR ranking on RB 2 as shown in Table I(c). Lastly, sector 3 is scheduled with the remaining RB 1 as shown in Table I(d).

(a)

	RB1	RB2	RB3
Sec 1	8	3	2
Sec 2	6	4	1
Sec 3	9	5	7

(b)

	RB1	RB2	RB3
Sec 1	8	3	2
Sec 2	6	4	**1**
Sec 3	9	5	7

(c)

	RB1	RB2	RB3
Sec 1	8	**3**	
Sec 2			1
Sec 3	9	5	

(d)

	RB1	RB2	RB3
Sec 1		3	
Sec 2			1
Sec 3	**9**		

TABLE I
Greedy scheduler for a sample SINR ordering.

We now derive the CDF of the SINR according to the RB rotation policy, i.e. $F_{\text{RB,rot}}(a) \triangleq P(\text{SINR}_{\text{RB,rot}} \leq a)$, in two steps. First, we compute the probability that, given nine i.i.d. SINRs, the fixed scalar a satisfies $\text{SINR}^{(n)} \geq a \geq \text{SINR}^{(n+1)}$ for $n = 0, \ldots, 9$. For each n, this probability is binomial

$$g_a(n) \triangleq \binom{9}{n} F_{\text{FFR}}(a)^{9-n}(1 - F_{\text{FFR}}(a))^n \,, n = 0, \ldots, 9. \tag{6}$$

Next, we find the probability for a sector to be assigned a RB with $\text{SINR}^{(n)}$, and we denote this probability as $r(n)$. Through careful combinatorial analysis, we summarize the values of $r(n)$ in Table II. We combine $g_a(n)$ and $r(n)$ to get

$$\begin{aligned} F_{\text{RB,rot}}(a) &= \sum_{n=0}^{9} g_a(n) \sum_{k=n+1}^{9} r(k) \\ &= F_{\text{FFR}}(a) \underbrace{\sum_{n=0}^{8} \binom{9}{n} F_{\text{FFR}}(a)^{8-n}(1 - F_{\text{FFR}}(a))^n R(n)}_{\triangleq \gamma(a)}, \end{aligned} \tag{7}$$

TABLE II
Values of $r(n)$ and $R(n)$.

n	r(n)	R(n)	n	r(n)	R(n)	n	r(n)	R(n)
1	1/3	2/3	4	11/126	37/126	7	1/18	1/9
2	1/6	1/2	5	43/630	71/315	8	1/18	1/18
3	5/42	8/21	6	37/630	1/6	9	1/18	0

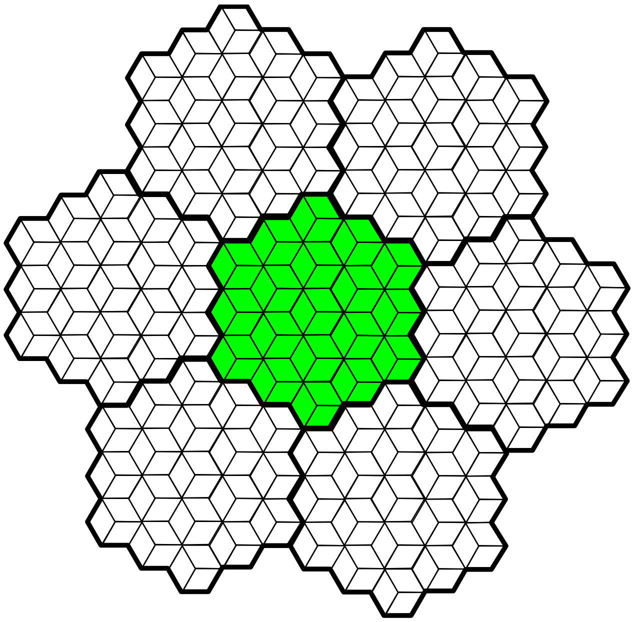

Fig. 4. 19-cell simulation environment with wrap around.

TABLE III
SIMULATION PARAMETERS.

Intersite distance (ISD)	500 m
Carrier frequency	2 GHz
Sampling frequency	15.36 MHz
FFT size	1024
Bandwidth	10 MHz
Occupied subcarriers	600
Subcarriers per RB	12
Center RBs C_c	26
Edge RBs C_e	24
Min. UE-BS distance	35 m
Path-loss model	-34.53 - 38 $\log_{10}(d)[dB]$, d in [m]
Shadowing std. dev.	8 dB
Horizontal antenna pattern	$A(\theta) = -\min\left[12\left(\frac{\theta}{70\deg}\right)^2, 20dB\right]$
Antenna boresight	
Fading model	Vehicular A [9, Sec. 4.2]
Cell center boundary	200 m from center
Center RB transmit power	10 dB
Edge RB transmit power	15 dB
Thermal noise power	-175 dB

where we define $R(n) \triangleq \sum_{k=n+1}^{9} r(k)$ (values shown in Table II). $\gamma(a)$ from (7) is the probability gain over the FFR scheme by performing greedy RB rotation. When $F_{\text{FFR}}(a) = 0.5$, $\gamma(a) = 0.55$. Hence, the median SINR a for FFR is exceeded by $1 - 0.5 * 0.55 = 73\%$ of the SINR values in the RB rotation.

Furthermore, note that the analysis on RB rotation can be applied for $n_{RB} > 1$ by replacing all instances of $F_{\text{FFR}}(a)$ by the CDF of the aggregate performance metric of each RB batch reported to the central scheduler. Hence, the median point for the aggregate performance metric for FFR is also exceeded by $\sim 73\%$ of the same aggregate performance metric for the RB batch rotation.

V. Simulation Results

In this section, we illustrate the performance of the proposed opportunistic cell edge selection scheme and compare its performance to the more conventional FFR scheme. Fig. 4 shows the layout of the system that we simulate. K users are dropped uniformly in each of the shaded sectors of the 19 cells in the center. We replicate the selection pattern in each of the six directions of the center 19-cell group to simulate interference. Performance statistics are collected for the center 19-cell group only. Other relevant simulation parameters are summarized in Table III.

Fig. 5(a) and Fig. 5(b) compare the SINR distributions of edge and center RBs respectively, under FFR, opportunistic cell edge selection, and the band rotation policy when $\text{RB}_{\max} = \infty$. Observe that the SINR distributions over center RBs are identical for each scheme, which satisfies intuition as our proposed schemes only operate on edge RBs. When K increases from 6 to 12, the performance of all schemes improved by about 5 dB. On the other hand, we see that the opportunistic cell edge selection scheme outperforms the band rotation scheme by about 7 dB, which in turn outperforms

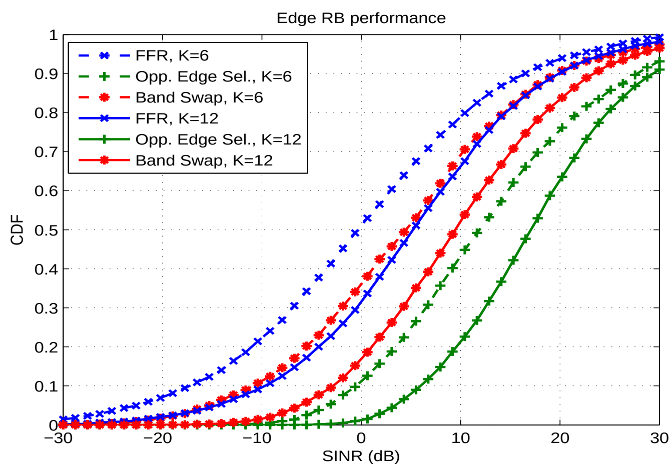

(a) Cell edge RBs SINR distributions.

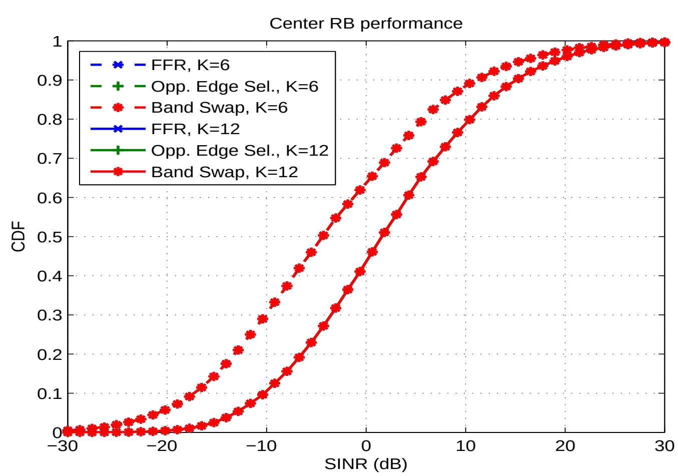

(b) Cell center RBs SINR distributions.

Fig. 5. Edge and center RB SINR distributions with 6 and 12 users per sector with $\text{RB}_{\max} = \infty$.

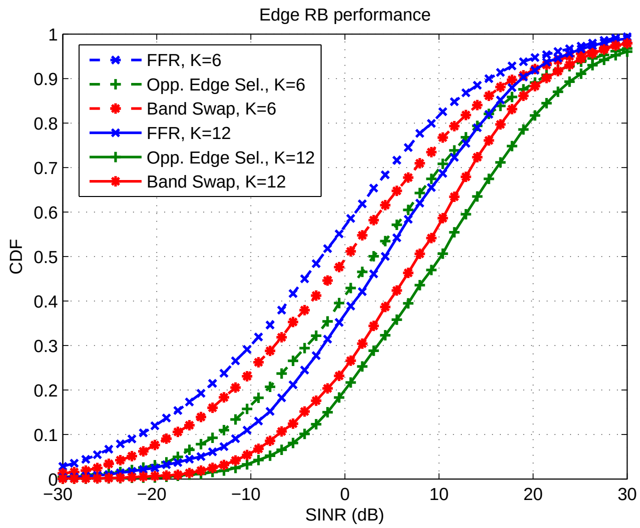

Fig. 6. Edge RB SINR distributions with 6 and 12 users per sector with $\mathrm{RB}_{\max} = 6$.

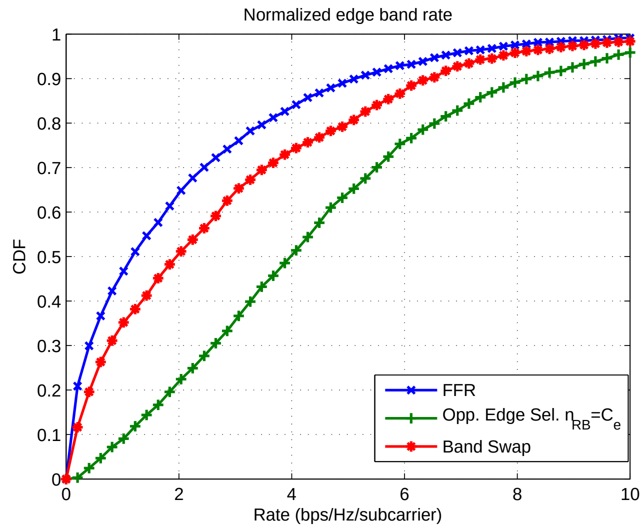

Fig. 7. Normalized edge band rate with $K = 6$ and $\mathrm{RB}_{\max} = \infty$.

FFR by about 4 dB. This is encouraging for a relatively small modification to the original FFR architecture. Note that when $a = 10$ dB, $F_{\text{FFR}}(a) \approx 0.69$ and $F_{\text{OCES}}(a) \approx 0.69^3 = 0.33$. Note also that when the number of UEs doubles from 6 to 12, performance for all three schemes improved by about 5 dB.

Fig. 6 compares the SINR distributions of edge RBs under conventional FFR, opportunistic cell edge selection, and the band rotation policy with $\mathrm{RB}_{\max} = 6$. We skipped the plot for the SINR distributions of center RBs as they are again, identical. The opportunistic cell edge selection scheme outperforms the band rotation scheme by about 3 dB, which in turn outperforms FFR by about 3 dB. The reduction in performance gain is attributed to the $\mathrm{RB}_{\max}$ restriction. The latter forces each sector to select users with less favorable channels, who generally have smaller range of fluctuations and leads to reduced performance gain. It is noteworthy that the band-rotation scheme still appreciably outperforms conventional FFR while incurring minimal backhaul cost.

Lastly, Fig. 7 compares the conventional FFR, the proposed opportunistic scheme for $n_{RB} = C_e$, and the band rotation scheme when $\mathrm{RB}_{\max} = \infty$. The x-axis measures the total rate of each edge band normalized by the number of subcarriers within the edge band. Note that relationship (5) still holds when comparing the FFR scheme and the opportunistic scheme with $n_{RB} = C_e$. This is because for a given edge band, the three aggregate achievable rates from the three sectors in a cluster are statistically independent. On the other hand, relationship (7) only approximately holds when comparing the FFR scheme and the band rotation scheme. The rate of 1 bps/Hz/subcarrier is the median rate for the FFR scheme. This rate is surpassed by about 64% in the band swapping scheme, less than the 73% predicted. The main reason for this discrepancy is insufficient frequency selectivity. As the band rotation scheme attempts to exploit frequency selectivity, it is intuitive that performance suffers when frequency selectivity is insufficient.

VI. Conclusions

In this paper, we proposed an opportunistic cell edge selection scheme in a sectorized cellular OFDMA downlink network. In this selection scheme, each RB is assigned to the rate-maximizing UE within a predefined cluster. Our proposed scheme results in a performance gain due to expanded multiuser diversity. Simulations show that the opportunistic selection scheme appreciably outperforms traditional FFR. We also proposed a backhaul-friendly variation by grouping RBs. As simulation shows, the band-rotation scheme also outperforms traditional FFR. As the proposed scheme requires relatively low overhead cost and decentralized operation, compared to other full base station cooperation strategies, it provides an attractive low-cost alternative solution for short-term implementation in next generation wireless cellular networks.

References

[1] M. K. Karakayali, G. J. Foschini, and R. A. Valenzuela, "Network coordination for spectrally efficient communications in cellular systems," *IEEE Wireless Commun. Mag.*, vol. 13, pp. 56–61, Aug. 2006.

[2] G. J. Foschini, H. Huang, K. Karakayali, R. A. Valenzuela, and S. Venkatesan, "The value of coherent base station coordination," in *Proc. Conf. Inf. Sci. and Sys. (CISS)*, Mar. 2005.

[3] B. L. Ng, J. S. Evans, S. V. Hanly, and D. Aktas, "Transit beamforming with cooperative base stations," in *Proc. IEEE Int. Symp. Info. Th.*, 2005, pp. 1431–1435.

[4] J. Zhang, R. Chen, J. G. Andrews, and R. W. H. Jr., "Coordinated multi-cell MIMO systems with cellular block diagonalization," in *Forty first Asilomar Conf. on Sig. Sys. and Comp.*, Nov. 2007, pp. 1669–1673.

[5] H. Zhang, N. B. Mehta, A. F. Molisch, J. Zhang, and H. Dai, "Asynchronous interference mitigation in cooperative base station systems," *IEEE Trans. Wireless Commun.*, vol. 7, no. 1, pp. 155–165, Jan. 2008.

[6] W. Choi and J. G. Andrews, "The capacity gain from intercell scheduling in multi-antenna systems," *IEEE Trans. Wireless Commun.*, vol. 7, no. 2, pp. 714–725, Feb. 2008.

[7] G. Li and H. Liu, "Downlink radio resource allocation for multi-cell OFDMA system," *IEEE Trans. Wireless Commun.*, vol. 5, no. 12, pp. 3451–3459, Dec. 2006.

[8] P. Viswanath, D. Tse, and R. Laroia, "Opportunistic beamforming using dumb antennas," *IEEE Trans. Inf. Theory*, vol. 48, no. 6, pp. 1277–1294, Jun. 2002.

[9] 3rd Generation Partnership Project, "Spatial channel mode for multiple input multiple output (MIMO) simulations (tr 25.996 v7.0.0)," Tech. Rep., 2007.